



Eidgenössische Technische Hochschule Zürich
Swiss Federal Institute of Technology Zurich

Magnetic Field Stabilization for Precise Qubit Calibration

Semester Thesis

Anqi Gong

February 22, 2022

Advisors: Dr. Daniel Kienzler, David Holzapfel

Department of Physics, ETH Zürich

Abstract

The magnetic field is an important resource for trapped ion quantum computing. However, due to the finite programming accuracy of power supplies, only discrete values of the magnetic field can be set. This limits the calibration precision of the qubits. In this thesis, we introduce how we achieved an almost continuous control of the magnetic field using a feedback mechanism consisting of an error-signal generating PCB and a PID lockbox. We further investigate whether this mechanism has any impact on stabilization by probing the qubit dephasing time.

Contents

Contents	ii
1 Introduction	1
1.1 The molecule experiment	1
1.1.1 The Beryllium hyperfine structure	1
1.1.2 Motivations and goals	2
1.2 Ramsey experiments	3
2 Setup	4
2.1 Connections	5
2.2 Control and Feedback	8
2.2.1 The EVIL and the power supply sense ports	8
2.3 Putting everything together	8
2.3.1 How to achieve finer control	9
2.3.2 Noise	9
3 Result	11
3.1 Comparison	12
3.1.1 Finer control step	12
3.1.2 Comparison – with or without stabilization	12
3.1.3 Comparison – with February result	12
3.1.4 Investigation of the causes	14
3.2 More experiments	14
3.2.1 Impact of wait time on different scan methods	14
3.2.2 Drift	15
3.2.3 Spin echo	15
3.2.4 Miscellaneous bugs	15
3.3 Future work	16
Bibliography	17

A Soldering and Testing	18
A.1 Soldering	18
A.2 Testing and debugging	19
B Schematics of the PCB	20

Introduction

1.1 The molecule experiment

The goal of the molecule experiment is to perform quantum logic spectroscopy (QLS) on the hydrogen molecular ion. QLS is an example of quantum metrology, which aims to perform high-resolution or highly sensitive measurements on physical parameters by exploiting quantumness (e.g., entanglement or squeezing). In our case, the experimental setup might be used in the future to determine fundamental constants or even explore physics beyond the standard model.

To be able to do that, we need to have full control over a single hydrogen molecular ion (the spectroscopy ion). This is done by co-trapping it with a well-controlled atomic beryllium ion (the logic ion). This mixed-species strategy enables sympathetic cooling on H_2^+ motional states using Be, and non-demolition measurements on states of the molecular ion, which works by transferring its internal state to a state of the logic ion for readout. Therefore, the full control over H_2^+ is conditioned on an excellent control over the logic ion. For more on QLS, see [5].

1.1.1 The Beryllium hyperfine structure

The ${}^9\text{Be}^+$ ion has a nuclear spin of $I = 3/2$, hence it possesses hyperfine structures. The total angular momentum $F = I + J$ is a good quantum number, which means that states with the same F have the same energy. In the presence of a weak external magnetic field B , the state $|F\rangle$ further splits into states $|F, m_F\rangle$, where m_F is the projection of F onto the external magnetic field (quantization axis). In the magnetic dipole approximation, the Hamiltonian which includes both the hyperfine and Zeeman interactions is

$$H = hA\vec{I} \cdot \vec{J} - \vec{\mu} \cdot \vec{B} = hA\vec{I} \cdot \vec{J} + (\mu_B g_J \vec{J} + \mu_N g_I \vec{I}) \cdot \vec{B}, \quad (1.1)$$

where A is the hyperfine splitting (in Hz) at zero applied magnetic fields. \vec{J} and \vec{I} are the electron and nuclear angular momentum operators. μ_B and μ_N are the Bohr magneton and nuclear magneton. g_I and g_J are the nuclear and Landé g -factors.

In the lab, we choose the magnetic field to sit at 4.5 G = $4.5 \cdot 10^{-4}$ T, which is in the weak-field regime but enough for the levels to split by more than usual light shifts caused by lasers.

For $J = 1/2^1$, the Hamiltonian can be solved analytically, resulting in the Breit–Rabi formula.

$$E_{|F, m_F\rangle} = -\frac{\Delta E_{hfs}}{2(2I + 1)} + g_I \mu_B m_F B \pm \frac{\Delta E_{hfs}}{2} \left(1 + \frac{4m_F x}{2I + 1} + x^2\right)^{1/2}, \quad (1.2)$$

where $\Delta E_{hfs} = A(I + \frac{1}{2})$ and $x = \frac{\mu_B(g_I - g_J)B}{\Delta E_{hfs}}$. For the beryllium ions, the minus sign applies to the $F = 1$ manifold, the plus sign applies to $F = 2$ manifold [4]. The zero-field splitting $A \approx -625$ MHz is negative, which means that the " $F = 2$ "-levels are energetically lower, as seen in figure 1.1a. We will mainly investigate the " 2211 transition" of $S_{1/2}$ between $|F = 2, m_F = 2\rangle$ and $|F = 1, m_F = 1\rangle$, in order to evaluate our stabilization mechanism. As can be seen from figure 1.1b (or by a rough calculation using the Breit-Rabi formula²), the transition frequency drops when the magnetic field strength is slightly raised³. The transition should sit at 1240.58 MHz when the magnetic field is set to 4.5 G, and the change rate is -2.1 MHz/G.

1.1.2 Motivations and goals

A fluctuating magnetic field will cause a change in the energy difference of the qubit levels, which results in the dephasing of the qubit. The magnetic field is produced by a coil (we call it the quantization coil). The current through the coil is driven by our power supply Agilent 66332a running in the current control mode. This power supply has a programming accuracy of 2 mA, which has been a headache for our molecule experiments. As we only have discrete control over the magnetic field, the resolution of the qubit transition frequency is limited to 20 kHz (see figure 3.1a). Our primary goal is to alleviate this issue. We do this by integrating a feedback and control system. We also expect this system to stabilize the magnetic field as an extra benefit.

¹For $^2S_{1/2}$ levels, $L = 0, S = 1/2$ and hence the electric quadruple interaction is zero, so the Breit-Rabi formula is fairly accurate.

²Again, please only focus on $B \leq 5$ G part. As B increases, the two states increase their energies by approximately $m_F g_I \mu_B B$. The state with $m_F = 2$ increases more but it's energetically lower-lying, so the gap shrinks.

³This fact will be useful when we verify the Stark shift.

Chapter 2

Setup

In order to stabilize the magnetic field, we utilize the feedback provided by an error-generating PCB board. The detail of soldering and testing the board is in Appendix A. In this chapter, I mainly discuss how to hook up the PCB box with the existing experiment and the control box EVIL.

The magnetic field we want to stabilize is induced by a coil, the current through which is provided by a voltage source (Agilent 66332A). We measure this current using a current sensor, then feed the sensed current into the PCB. This sensed current is converted into a voltage and compared to a reference. The difference is the output error signal of the PCB and it is forwarded to the EVIL. The EVIL gives out a feedback signal, which is used for counteracting the fluctuation of voltage in our power supply.

In the remaining section, we recapitulate how the error signal is generated and how to estimate it.

The conversion ratio of our current sensor (LEM IT 60-S Ultrastab) is 1:60. Assume the current through the coil to be I_{out} ($I_{out} \approx 5A$ in our case). We wind the wire eight times through the current sensor, then the sensed current by the current sensor is $I' = I_{out} \cdot 8/60$.

The ultra-high precision resistor (R303) that converts the sensed current to a voltage has a resistance of 10Ω . When directly measuring it after it was soldered to the board, however, 7.8Ω is found. The reason behind this, is that the current needs to go through two low pass filters before reaching the voltage buffers ($U300A/B$)¹, and the resistors from those low pass filters (RC circuits) change the effective resistance. A coarse estimation of which is $\frac{1}{1/R303+1/(R301+R302+R304+R305)} = \frac{1}{1/10+1/64} = 8.64\Omega$. The residue may be due to other components connecting to the GND. The schematic of this part can be found in Appendix B Differential Amplifier.

When we connect the PCB to the current sensor and turn on the power, we

¹If the buffers are put in front of the low-pass filters, it should indeed be 10Ω . But new noises may be introduced. The low-pass filters are removed from the new design.

infer that the effective resistance R is around 3Ω . This change is due to the resistance of the current sensor. Though it's not possible to predict the exact value of R in advance, it is confirmed to be stable in time².

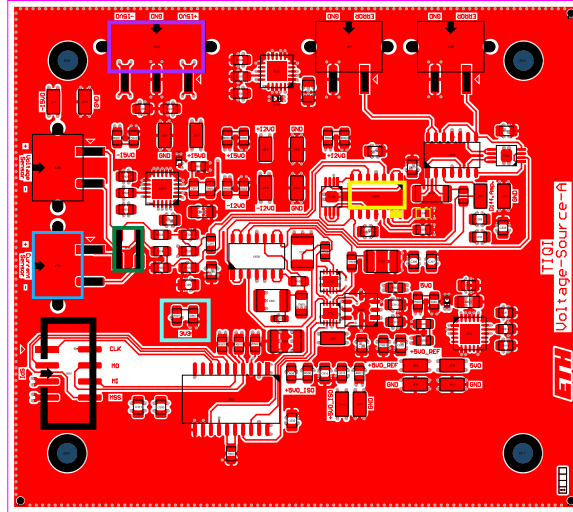
The converted voltage $I'R$ is then amplified 202 times and compared to a reference V_{ref} (Appendix B Reference Subtraction). This reference is generated by a pair of coarse/fine DACs, through the relation

$$V_{ref} = 200V_{DAC_{coarse}} + V_{DAC_{fine}}. \quad (2.1)$$

The two DACs can be set separately using the Raspberry Pi, and their values must both be an integer multiple of $V_{max}/2^{16}$, where $V_{max} = 1.9898V$. In conclusion, the output error signal of the PCB is

$$V_{err} = 200V_{DAC_{coarse}} + V_{DAC_{fine}} - 202 \cdot I'R. \quad (2.2)$$

Figure 2.1: Layout of the top layer of the PCB. Green box: the ultra-high precision resistor R303. Purple box: the power connector of the PCB. Cyan box: the resistor R907 and the diode D907 for the indication of 3.3V. One of them should be desoldered [2]. Yellow boxes: the operational amplifier U300 and the two pins to be shorted, and the resistor R306 to be desoldered [2]. Blue box: the port J302 where the sensed current comes in.



2.1 Connections

The PCB is enclosed by a metal box, which aims to shield the outside electromagnetic field. Specifically, we placed the PCB on the back side of the lid (figure 2.2b).

²This is for a short period. For a longer period, the thermal effect on the PCB should be taken into account.

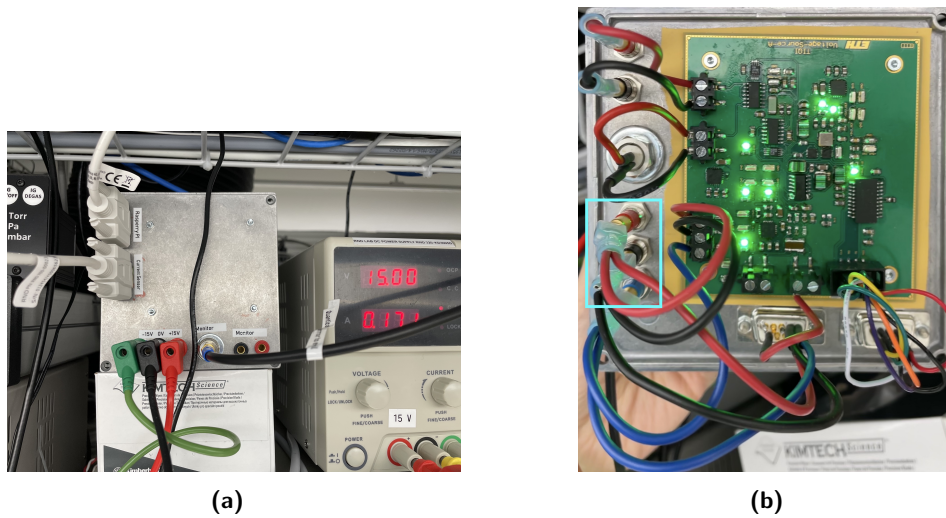
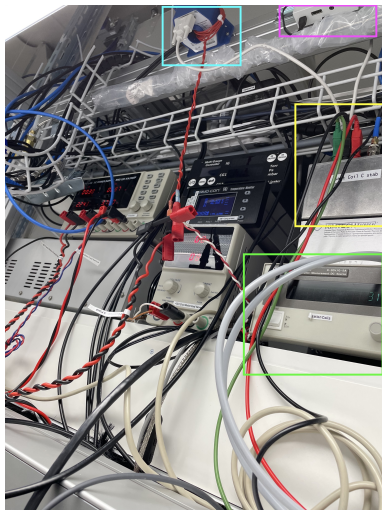


Figure 2.2: The front and backside of the lid. (a) Front side of the lid. Green/black/red banana plugs for $-15\text{V}/0\text{V}/15\text{V}$. Two serial connectors for Raspberry Pi and the current sensor. One BNC connector for forwarding signal to EVIL. A pair of banana sockets are not used in this picture, but they have been used for monitoring signals. (b) The backside of the lid is where the PCB is screwed to. A thermal pad is put in between. The cyan box is where the power lines split into two, powering both the PCB and the current sensor.

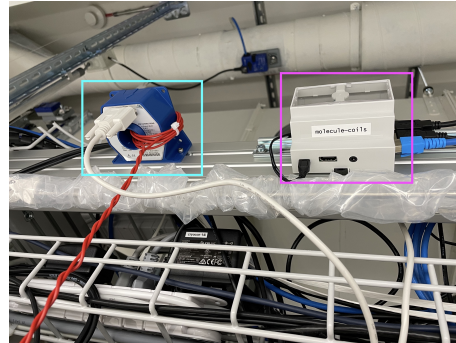
Both the PCB and the current sensor require $\pm 15\text{V}$ and GND power input. To provide that, we use two single-polarity power supplies (RND 320-KD3005D) to emulate a dual-polarity one. This is done by connecting the - terminal of the first power supply to + of the second one. Then the + terminal of the first one provides $+15\text{V}$, the - terminal of the first one (as well as the + port of the second one) becomes GND, and the - terminal of the second one functions as -15V . We took the advice from Ilia to leave the GND terminals unused.

As can be seen from the back side of the lid, each power line is split into two, one supplies power to the PCB, and the other is connected to the serial port of the current sensor (see figure 2.2b). Here one should be aware that the output return and the GND is internally connected in the current sensor. So either pin 1 (output return) or pin 4 (GND) of the serial port should be used, but not both! [3] Otherwise a ground loop will occur and cause large noise on the error signal. In our case, we soldered GND to pin 1 (output return), and J302 + to pin 6 (output). The connection from J302 - to pin 4 (GND) should NOT be made.

The other serial port is for communication with the Raspberry Pi. Its connection to the PCB has already been specified in the previous report [1], and will be omitted here. We hereby report an unexpected behavior of the diode D907. This LED is dim when the connection to Raspberry Pi is first plugged in, and gradually lights up in ten minutes. Since this LED is unable to indi-



(a)



(b)

Figure 2.3: Connections in the lab. (a) The connection of the box (yellow), the Raspberry Pi (purple), the current sensor (cyan) and the power supply (green). (b) Focusing on the current sensor (cyan) and the Raspberry Pi (purple).

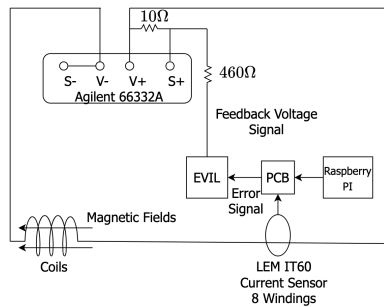


Figure 2.4: A simplified diagram showing the relationship between each component. The current the power supply provides passes through the coil and produces the magnetic field to be stabilized. This current is measured by a current sensor and the value is compared to a reference value set by us through the Raspberry Pi. This difference (error signal) is fed into the EVIL, which created a feedback voltage to be put alongside with the power supply.

cate whether the communication is established or not, we simply desoldered it.

The two ports J400/401 produce the identical output signal. We forward one to a solder-type BNC connector and then to the EVIL, and the other to banana connectors.

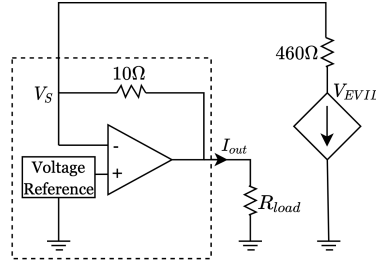


Figure 2.5: The part in the dotted line is a simplification of the feedback mechanism inside the power supply, when it's in the voltage control mode and sense ports are used. The sensed voltage V_S is stabilized to a voltage reference (e.g. 3.4V in our case). The current sensor, the PCB, and the EVIL are together abstracted as a Current Controlled Voltage Source that provides V_{EVIL} depending on the measured current. The resistance of the coil and the wires are modeled as R_{load} .

2.2 Control and Feedback

2.2.1 The EVIL and the power supply sense ports

The EVIL is a PID lockbox used in TIQI experiments. It takes the error signal generated by the PCB and outputs a voltage, which is used to counteract the fluctuations of the current. So the voltage it outputs (V_{EVIL}) is a function of the current in the circuit (I_{out}), see figure 2.5. We therefore model the EVIL feedback mechanism as a Current Controlled Voltage Source.

On the other hand, when the power supply is in the voltage control mode, and the sense ports are used. The power supply has an internal feedback mechanism to stabilize the sensed voltage (V_{sense}). A simplified version is shown in the dotted box of the figure 2.5. We short-circuit the sense minus port (S-) with V- using contacting washers, so that they are both connected to the lab GND. Moreover, we insert a resistor (10Ω) between S+ and V+ while putting a resistor (460Ω) in series with V_{EVIL} , so that we are able to adjust the feedback strength of the EVIL. A circuit analysis shows

$$\begin{aligned} V_S - I_{out} \cdot 10\Omega &= I_{out} \cdot R_{load} \\ V_{EVIL} - V_S &= I_{out} \cdot 460\Omega, \end{aligned}$$

which is equivalent to

$$\frac{V_S}{10\Omega} + \frac{V_S - V_{EVIL}}{460\Omega} = \frac{R_{load} \cdot I_{out}}{10\Omega}. \quad (2.3)$$

We can see that, if we increase the ratio $\frac{460\Omega}{10\Omega}$, V_{EVIL} will affect I_{out} less.

2.3 Putting everything together

The figure 2.4 shows a schematic of the complete feedback setup. The power supply Agilent 66332A is now set to be in the voltage control mode. The cur-

2.3. Putting everything together

rent it provides passes through the coil and produces the magnetic field to be stabilized. This current is measured by a current sensor and the value is compared to a reference value set by us through the Raspberry Pi. This difference (error) is fed into the EVIL and a compensating voltage is created and put alongside with the power supply.

Our Raspberry Pi server has been integrated into Ionizer as a plugin³. Through setting `quantcoil_stab.voltage_coarse/fine`⁴, the reference voltage can be adjusted.

Figure 2.6: Ionizer Plugin page, where parameters for the molecule experiments can be set. The new fields we add are `quantcoil_stab.voltage_coarse` and `quantcoil_stab.voltage_fine`.



2.3.1 How to achieve finer control

As we have mentioned in the beginning, we want to achieve a finer control over the magnetic field, apart from stabilizing it. If we adjust $V_{DAC_{fine}}$, we wish to see an almost continuous change in the magnetic field strength. This can be achieved by increasing the ratio of the two resistance, e.g. $\frac{460\Omega}{10\Omega}$, or simply decreasing the gain of EVIL. On the other hand, we want to be more sensitive to the fluctuation in the current that we want to stabilize. To do that, we can increase the winding number, as long as the total current going through the current sensor does not exceed the measurement range of the current sensor.

2.3.2 Noise

People who also want to use this box in the future might find this subsection useful.

We have encountered several sources of noise when setting up the experiment:

1. The EVIL gives out both a feedback voltage and a ground reference. This ground should not be connected anywhere else. Otherwise, a ground loop will be created.

³For the code, see `molecule-coils-server.py` and `Quant.coil.C_stab.py` in <https://gitlab.phys.ethz.ch/tiqi-projects/molecule/magnetic-field-coils>.

⁴They correspond to the two parameters $V_{DAC_{fine}}$ and $V_{DAC_{coarse}}$.

2.3. Putting everything together

2. We used to see an asymmetric saw-tooth noise, with a peak at 15.2kHz for current sensor IT 200-S and a peak at 14.4kHz for IT 60-S. The reason behind it, as we have mentioned, is the ground loop caused by using both the output return and GND of the current sensor.
3. As can be seen in figure 2.3a, the current sensor is fixed at the top. The long dangling wire going up and down in order to pass through the current sensor has caused large noise. We believed that this noise was due to the large loop experiencing magnetic induction caused by a large magnet in our room. After twisting the wire together, the noise is reduced drastically.
4. As discussed in creating a dual-polarity power supply, the GND terminals are left unused. If they were connected to the + terminal of the first power supply (or the - terminal of the second), potential ground loops might occur.

Chapter 3

Result

After setting up the stabilization mechanism, we proceed to investigate its performance.

The first step is to find the correct $V_{DAC_{coarse}}$. For the very first time, we recommend plugging in the oscilloscope and monitoring the output of the PCB while manually tuning $V_{DAC_{coarse}}$ through the Ionizer plugin interface. In our system, we do this until the output of the PCB reaches an RMS of about 200meV. Then in the Ionizer Beryllium 2211 π pulse calibration interface set the transition frequency to be 1240.58MHz. For a coarse estimation, we set the amplitude of the π pulse to be 100% and the time to be $4\mu s$. Then we fix $V_{DAC_{fine}} = 1V$ and scan $V_{DAC_{coarse}}$ for a span of $0.01V^1$. Fit the dip and obtain the corresponding $V_{DAC_{coarse}}$.

Keep setting the transition frequency to be 1240.58MHz, the second step is to scan the entire range $0V - 1.9898V$ of $V_{DAC_{fine}}$ and fit the dip, with amplitude and the time of the π pulse being 45% and $60\mu s$. With a π pulse of lower amplitude and longer time, we can have a narrower transition², thus calibrating the magnetic field more precisely.

Since the microwave pulses affect the transition frequency (Stark shift), the third step is to scan the 2211 transition frequency with 100% π pulse. Subsequently, we can likewise characterize all the π or $\pi/2$ pulses for other relevant transitions.

¹Recall both $V_{DAC_{coarse}}$ and $V_{DAC_{fine}}$ have max 1.9898V. And $V_{DAC_{coarse}}$ contributes 200 times of the $V_{DAC_{fine}}$.

²Fixing the transition frequency and $V_{DAC_{coarse}}$. Sweep and fit for $V_{DAC_{fine}}$ using first a 100%, $4\mu s$ π pulse and then a 45%, $60\mu s$ π pulse. Not only is the line-width of the latter smaller, but also the line-center becomes smaller too (by $0.02V$ in our case due to Stark shift). The Stark shift of the internal state transition frequency ω_a is $\delta\omega_a = 2\Omega_R^2\bar{n}/\Delta$, where $\Delta = \omega_a - \omega_L < 0$ in red side-band transition. When decreasing amplitude, Ω_R decreases and thus ω_a increases, which means $V_{DAC_{fine}}$ decreases.

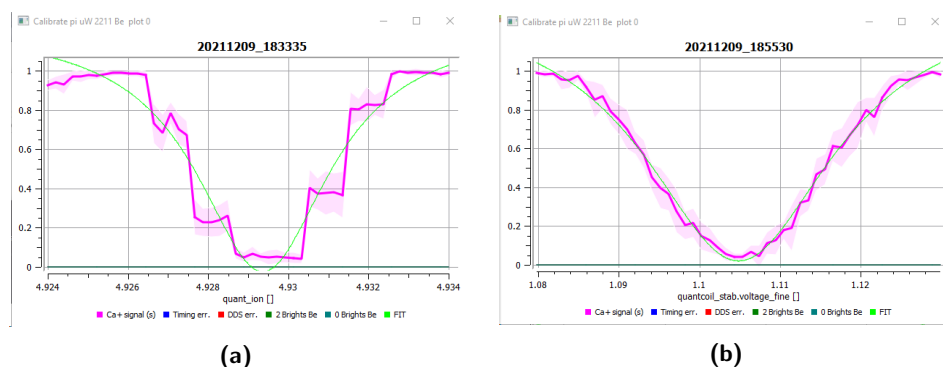


Figure 3.1: Fixing the resolution problem. (a) The current power supply (Agilent 66332A) has programming accuracy 10mV and 2mA, this manifests itself in the "steps" (current range from 4.924A to 4.934A, i.e., span 0.01A). (b) After the stabilization mechanism was integrated into the experiment, a rather smooth transition could be achieved. This range of the $V_{DAC_{fine}}$ corresponds to a current range from 4.925A to 4.934A, i.e. span 7mA.

3.1 Comparison

3.1.1 Finer control step

As can be seen in figure 3.1b, we can now achieve an almost continuous control of the magnetic field. This stabilization mechanism might benefit groups that deal with large magnetic fields but are limited by the programming accuracy of their power supply.

3.1.2 Comparison – with or without stabilization

We performed 2211 transition characterizations with and without our stabilization mechanism (figure 3.1b, 3.1a). The simplest comparison is their line width, where no improvement was seen. We turned to the Ramsey experiment for better comparison. However, there was still no improvement (figure 3.2a, 3.2b).

3.1.3 Comparison – with February result

We want to find out why our stabilization mechanism did not help. There was a characterization performed by Daniel on this power supply nine months ago (February 2021). The Ramsey results can be seen on the left of the figures 3.3a and 3.4a. On the right side of those figures, the Ramsey results performed nowadays by us with same setting (without stabilization) are shown. Our power supply performs a lot worse than nine months ago in terms of coherence. The causes are still under investigation, but the stabilization mechanism is not one of them.

3.1. Comparison

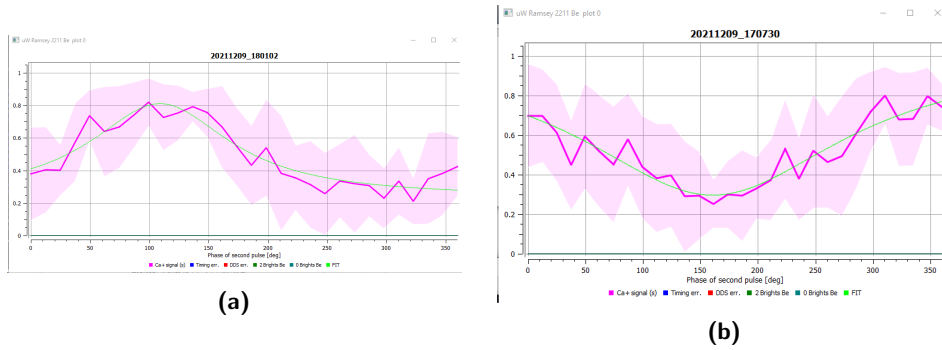


Figure 3.2: Ramsey experiments Plotting the transition probability against the phase of the second pulse (or equivalently, the phase difference between the two pulses). Both insets were taken for $T = 500\mu\text{s}$, 10 repetitions and 30 data points. (a) Without stabilization. (b) With stabilization. Stabilization has neither improved nor worsened the coherence.

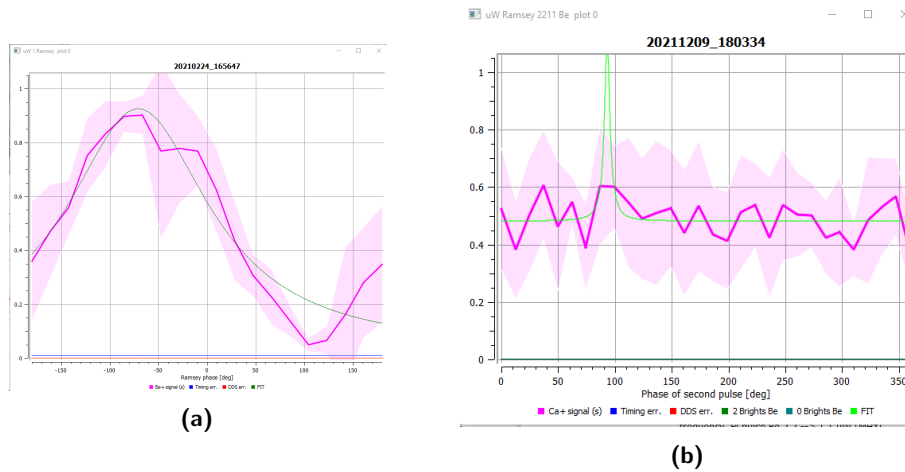


Figure 3.3: Ramsey experiments. Both insets were obtained for $T = 1\text{ms}$, with results averaged over 10 repetitions. (a) Result of February (nine months ago). (b) Now without stabilization. The coherence is a lot worse nowadays.

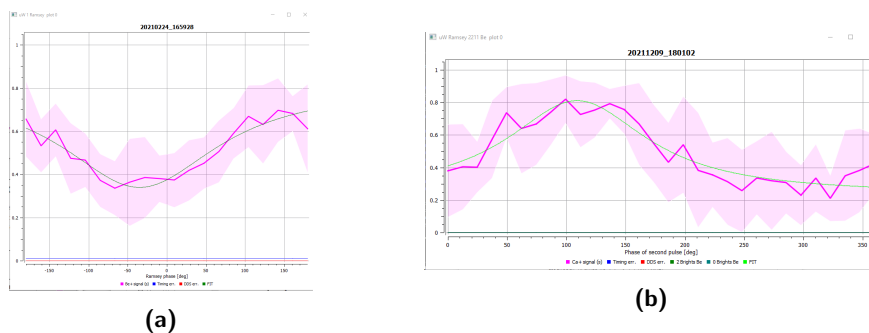


Figure 3.4: Ramsey experiments. Both insets were results averaged over 10 repetitions. (a) February $T = 3\text{ms}$. (b) Now $T = 500\mu\text{s}$ without stabilization. Coherence is about 6 times worse.

3.2. More experiments

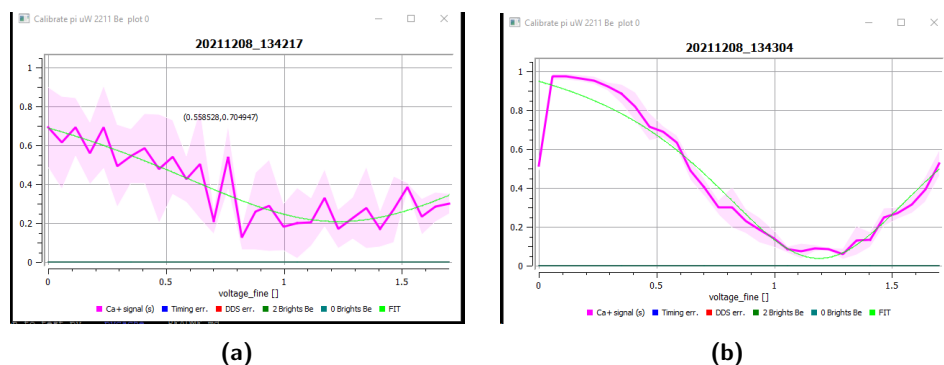


Figure 3.5: Linear vs scatter scan. Both figures were obtained by setting the pulse amplitude to 35% and the pulse time to 400s. (a) Scatter scan with 0.1s wait time. (b) Linear scan with 0.1s wait time.

3.1.4 Investigation of the causes

We noticed an unusual vibration of our power supply. To exclude the possibility of vibration worsening the magnetic field, we borrowed another power supply (TTI PL155) and did the same test with it (no stabilization connected), but no improvement was seen.

We also have tried to turn off the Penning magnet in our room and again no improvement.

The frequency analysis of the PCB output signal didn't show any suspicious noise peaks. Maybe the noise was not from the power supply, but was something that affected the magnetic field inside the coil directly.

We didn't do any further investigations as coherence is not our main concern for now. Also, the loss of coherence time might not have anything to do with the stabilization, but most probably was due to other things in the lab changing during these months.

3.2 More experiments

This section contains some more experiments we've done. These are not directly related to our two goals (stabilization and finer control). I wrote them down in case anyone in the future uses this stabilization mechanism and wants to compare.

3.2.1 Impact of wait time on different scan methods

When sweeping $V_{DAC_{coarse}}$ with 0.1s wait time using scatter scan (figure 3.5a), we observed large oscillations, and no well-formed dip. While the linear scan (figure 3.5b) gave a smooth transition. The reason is that a 0.1s wait time is too short for the EVIL to adjust itself to the target value. The wait time was chosen to be 0.5s in the end.

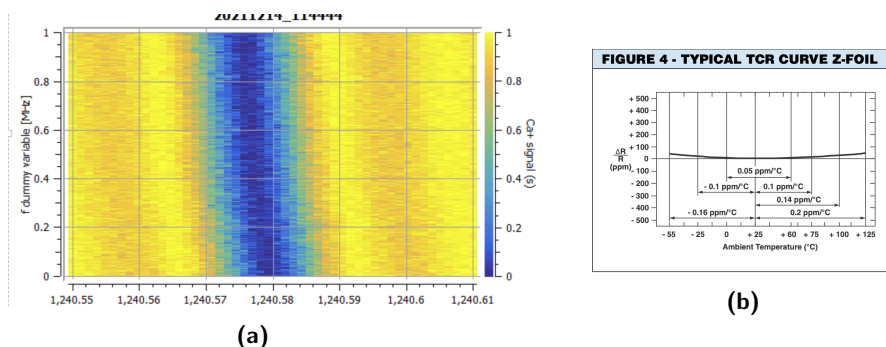


Figure 3.6: Transition drift and its explanation. (a) Be 2211 transition drift over an hour with π pulse amplitude 45%, time $65\mu\text{s}$. (b) The TCR curve of the ultra-high precision resistor (R303) taken from its datasheet.

3.2.2 Drift

Figure 3.6a shows that the 2211 transition drifts about 4kHz in an hour (performed by David). The drop in frequency indicates an increase in current. While V_{target} remains the same. A possible explanation is a decrease in effective resistance due to heating. Referring to the datasheet (figure 3.6b) of the ultra-high precision resistor (R303), it has a temperature coefficient of resistance (TCR) of $\pm 0.05\text{ppm}/\text{C}^\circ$ (0C° to 60C°). This will not be an issue as long as a re-calibration is done once in a while.

3.2.3 Spin echo

The spin echo technique is used to cancel the low frequency noise ($\omega \ll 2\pi/T$) in the qubit phase accumulated during its free evolution.

Comparing Ramsey results for $T = 500\mu\text{s}$ of spin echo to the plain version, we think the primary component of the noise that worsens our magnetic field should be in kHz range or below.

3.2.4 Miscellaneous bugs

We have encountered server-side crashes several times saying "too many open files" and "object of AD5541 is not JSON serializable". This was due to inappropriate server-side exception handling and this issue has already been resolved by the latest version of the tiqi-plugin package. An upgrade should solve these kinds of errors.

After we upgraded the tiqi-plugin and restarted the server and loaded the previous value of $V_{DAC_{coarse}}$ and $V_{DAC_{fine}}$ into Ionizer, we saw a sudden drop of the current from 4.92A to 4.11A and the power supply jumped from the voltage control mode to the current control mode. We have developed a solution to put everything back to locked again.

On the EVIL side, decrease the range to 0 and decrease/increase the center

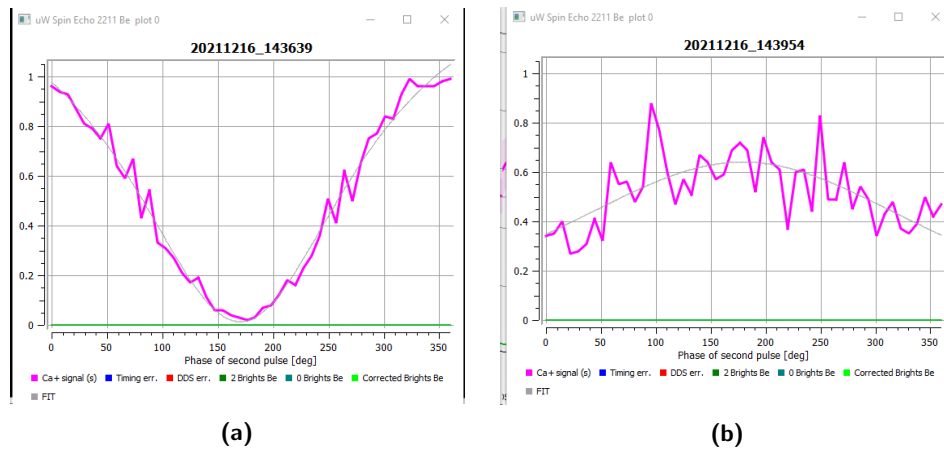


Figure 3.7: Spin echo experiments, where a π -pulse is inserted between two $\pi/2$ -pulses separated by time $2T$. **(a)** $T = 500\mu\text{s}$, we can see perfect coherence. **(b)** $T = 5\text{ms}$, still some coherence left. Compared to 3.2a, we can increase the coherence time from $500\mu\text{s}$ to $T = 5\text{ms}$ with spin echo.

and we will see the current go up/down (when adjusting the center, make sure that the Evil output is higher than zero).

Then on the power supply side, adjust its voltage until the current returns to 4.9A and the mode is back to voltage control³.

3.3 Future work

The original design of the box includes a temperature controller to be placed on the lid. We did not use it as the temperature stability is not very important for us. However, incorporating the temperature controller might help with alleviating the drift in the transition frequency.

Some mistakes in the PCB design has been found, for example the low-pass filters after the ultra-high precision resistor, the others are marked in the figure 2.1 and mentioned in [2].

Though we have ruled out several possibilities. The reason of the decrease in coherence time compared to February 2021 is still unclear.

Whether the feedback mechanism (the PCB and the EVIL) can potentially stabilize the magnetic field is unpredictable. One reason is because the PCB will itself induce some noises [2], the other is that we don't know whether this feedback mechanism and the one within the power supply (figure 2.5) could together function better or not.

³If the power supply were in current control mode, stabilization won't have any effect.

Bibliography

- [1] Tenzan Araki. *Error Signal Generation for Ultrastable Voltage Source*. Semester Thesis, ETH Zurich, 2021.
- [2] Giorgio Fabris. *Error Signal Generator for Ultrastable Voltage Source*. Semester Thesis, ETH Zurich, 2021.
- [3] Christa Flühmann. *Encoding a qubit in the motion of a trapped ion using superpositions of displaced squeezed states*. PhD thesis, ETH Zurich, 2019.
- [4] Hsiang-Yu Lo. *Creation of squeezed Schrödingers's cat states in a mixed-species ion trap*. PhD thesis, ETH Zurich, 2015.
- [5] P. O. Schmidt, T. Rosenband, C. Langer, W. M. Itano, J. C. Bergquist, and D. J. Wineland. Spectroscopy using quantum logic. *Science*, 309(5735):749–752, 2005.

Soldering and Testing

A.1 Soldering

Instead of using a reflow oven, I soldered everything by hand. I wrote down my experience in case others need to solder this type of PCB in the future. Hard things should be done first, as at that time there is still plenty of space to operate. This includes the voltage regulators and the ICs. Then proceed with the capacitors and resistors, and lastly the headers/connectors.

To solder the voltage regulators, put the board onto the pre-heater and turn the temperature to around 160C° . Put tin onto the pads on the backside of the regulator. Coat the pads on the PCB with flux, then align the voltage regulators with the pads. Press the diagonal corners hard using tweezers while turning on the heat gun at 250C° . The heat gun should blow air perpendicularly to the PCB. Stop until you feel the regulator sinks into the flux blob and slips onto the right position. Excessive tin will be repelled thanks to the flux and can be removed easily. You can check whether all four corners cling to the PCB by using a microscope. Solder the three super tiny diodes (D800-D802) near the three regulators only after a confident check, because the heat gun could blow them away even when they were soldered. The direction of the diodes can be seen using a magnifier or a camera. One end has a white bar on it as drawn on the PCB layout 2.1. Another alternative is to measure the diode using a multi-meter.

The dot on the ICs should align with the black triangle on the layout 2.1. Solder one pin first to fix the IC to the board. Then with a little bit of flux and a suitable amount of tin at the tip of the soldering iron, slide the iron along each edge while pressing the IC using tweezers.

Capacitors, resistors, and diodes share the same soldering methods. Apply tin to one end of the pad on the PCB and put the iron there to keep it melted, then tweeze the component into the tin, and apply tin to the other end.

Tips: clean the tip of the soldering iron regularly using tin to protect it from oxidation, and clean the flux residue on the PCB as it can potentially erode

the board.

A.2 Testing and debugging

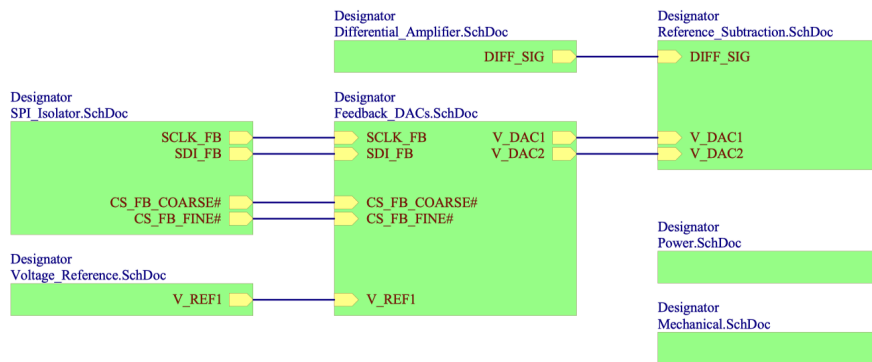
Before turning on the power, double-check the directions of all the diodes. Scrutinize all the ICs to see whether there are any suspicious short-circuits between pins or any aloft pins. For the former, a check using the multimeter is required. Any excessive tin can be removed either with the help of the flux or the desoldering braid. For the latter, you might use the heat gun to blow the IC to a horizontal position.

When connected to power, all LEDs except the one for the Raspberry Pi should light up, indicating a correct voltage distribution. If this does not happen, the most probable error happens at the voltage regulators (U800-U802). You can measure the voltage difference of input/output pins to the GND (yellow borders of the PCB) to see whether their values match the schematics. In case not, either not all corners of the regulator cling to the PCB or not enough tin was applied.

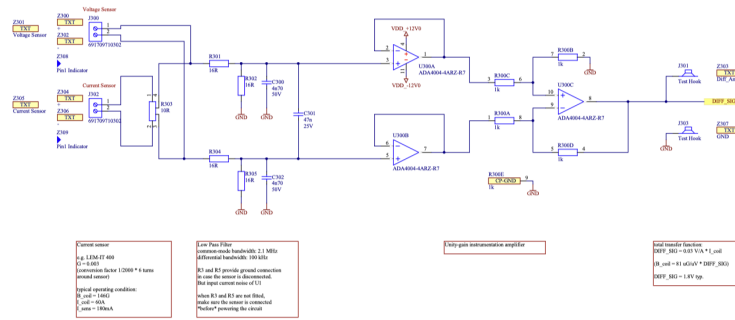
In case you still cannot solve the bug, ask Ilia for help.

Appendix B

Schematics of the PCB



Differential Amplifier



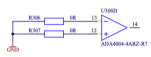
Current sensor
 $R_1 = 1.04k\Omega$ (1%)
 $R_2 = 0.40k\Omega$ (1%)
 $R_3 = 1.04k\Omega$ (1%)
 $R_4 = 1.04k\Omega$ (1%)
 $R_{sense} = 100m\Omega$

Gain
 $G = 10$
 $R_{sense} = 100m\Omega$
 $R_1 = 1.04k\Omega$ (1%)
 $R_2 = 0.40k\Omega$ (1%)
 $R_3 = 1.04k\Omega$ (1%)
 $R_4 = 1.04k\Omega$ (1%)

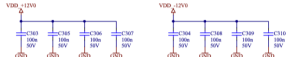
Differential instrumentation amplifier

Final output
 $DIFF_SIN = 10 \cdot (V_{IN1} - V_{IN2}) + 1.5V$
 $R_{sense} = 100m\Omega$
 $DIFF_SIN = 1.5V$ (typ)

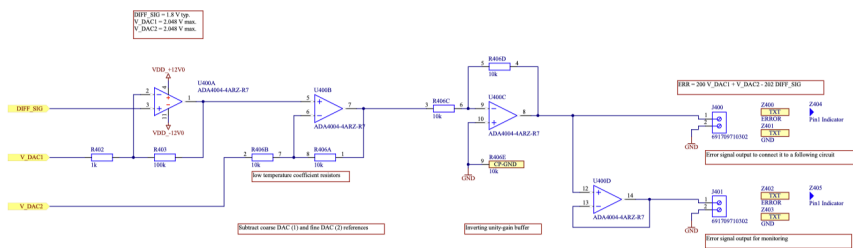
Available parts



Decoupling



Reference Subtraction



DIFF_SIN1 = 1.5 V (typ)
 $V_{DAC1} = 1.666 V$ (nom)
 $V_{DAC2} = 2.666 V$ (nom)

Subtract DAC (1) and the DAC (2) references

Inverting unity-gain buffer

$DIFF_SIN = 10 \cdot (V_{IN1} - V_{IN2}) + 1.5V$

Error signal output to connect to a following circuit

Error signal output for monitoring

Decoupling



